PREMIXED TURBULENT FLAME PROPAGATION IN MICROGRAVITY

Annual Report
for the period March 1996 - July 1997
Grant No. NAG3-1610

Summary

The research work carried out under this project during the performance period indicated above was described in details in a series of papers, including a paper presented at the Fourth International Microgravity Combustion Workshop held in Cleveland. These papers are attached as appendices to this report and constitutes the annual report under this grant.

Proceedings of Fourth International Microgravity Combustion Workshop, pp 155-160, NASA CP 10194.

TURBULENT PREMIXED FLAME PROPAGATION IN MICROGRAVITY

S. MENON*, M. Disseau+, V. K. Chakravarthy+, and J. Jagoda*
Georgia Institute of Technology
School of Aerospace Engineering
Atlanta, Georgia

Introduction

The structure and propagation characteristics of turbulent premixed flames have been investigated for some time. For example, the turbulent flame speed has been typically estimated in terms of the laminar flame speed S_L and the local turbulence intensity u'. However, the exact form of the functional relation: $u_T/S_L = f(S_L, u')$ has not yet been determined although various models have been proposed (ref. 1). A key reason for this uncertainty is the inability to experimentally resolve all scales of motion that could contribute to the wrinkling of the premixed flame and hence, to an increase the effective burn speed. In a typical high Reynolds number flow, the small scales are impossible to resolve in an experiment (e.g., using LDV). However, turbulent fluctuations at the small scales (e.g., Kolmogorov scale) could be resolved if the Reynolds number is reduced (for example, by reducing the flow velocity). A flow field that provides sustained turbulent flow in a relatively low Reynolds number is Couette flow. It has been shown in past studies that stationary turbulent Couette flow could be achieved at Reynolds number as low as 1800. Once combustion is included, however, the large-scale turbulent stresses responsible for momentum transport can be overwhelmed by the buoyant stresses in 1g. Since this phenomenon is not present in realistic high Reynolds number devices, a microgravity environment is required to suppress the buoyancy effects while still maintaining reasonable operating pressure, temperature and observable scales at all sizes.

This paper summarizes the results obtained so far in this study. Both experimental and numerical studies are being performed to investigate turbulent premixed flames. The experiments so far have focused on characterizing the turbulent flow field in this new Couette flow facility. A major reason is that the current device has been designed to fit inside the NASA Lewis 2.2 s drop tower rig (ref. 2). As a result, this facility is much smaller than the facilities used in the past (ref. 1-3). For example, the current length to gap ratio is 14 compared to 30-158 of the earlier devices (refs. 3-7). In addition, the current device operates in a closed loop, i.e. turbulent flow is forced to reenter the test section whereas earlier devices transition the flow from laminar to turbulent. Thus, it is essential to quantify the turbulence properties of this device.

The numerical study employs large-eddy simulation (LES) technique. In this approach, all scales of motion larger than the grid resolution is captured in the simulation without modeling and only scales smaller than the grid are modeled. A localized dynamic subgrid model for the subgrid kinetic energy is used in this study to model the subgrid stresses. However, since the flame thickness is much smaller than the typical grid resolution employed in LES, conventional LES of species equations will not capture the true features of the flame. Here, a new subgrid combustion methodology has been developed to simulate the burning process within the small scales (refs. 8,9). In this approach, the local laminar burning, wrinkling due to the local subgrid turbulence and volumetric expansion due to heat release are explicitly included within the subgrid scales. This approach also predicts the local (turbulent) burn speed provided the local turbulent field is known. The experimental data on the turbulence provides the required information to (hopefully) accurately evaluate the propagation characteristics of turbulent premixed flames using this simulation approach. Thus, the present study combines the capabilities of both experimental and numerical methods to investigate premixed flames.

Experimental Facility

The experimental device shown in Fig. 1 consists of a continuos Mylar belt moving in opposite directions over a series of rollers, two of which drive the belt while four are used to adjust the spacing in the test section. It is driven by an adjustable DC motor connected to the drive roller by a set of pulleys and a v-belt. To prevent belt walking and to ease the insertion of a new

Work funded by NASA Grant NAG3-1610
* Professor
+ Graduate Research Assistant

belt, a set of tensioning screws help position the far roller. Two plates are placed on the outside of the belt to reduce belt vibration. The Reynolds number for the device, Re_h, can be changed by either changing the speed of the belt, U_{belt}, or by changing the belt spacing, h. The device is surrounded by a Plexiglas box to prevent any external influence on the flow without disturbing optical access to the experiment.

The velocity flow field was mapped with a TSI 9100-7 two component laser Doppler velocimeter, which uses the 514.5 nm and 488 nm wavelengths of an 5 watt Ar^+ laser. After going through an expander and focusing using a 14 mm aperture lens, with a 750 mm focus, the probe volume was 0.13 mm in diameter and 1.3 mm long. The system was used in back scatter mode. The output signals were analyzed by a TSI IFA656 digital burst correlator, which can cope with lower signal to noise ratios than a traditional counter. One beam of each pair was frequency shifted by a Bragg cell to allow for measurement of negative velocities. Sub-micron TiO_2 particles were used to seed the flow. After passing though a fluidized bed, TiO_2 laden air is inserted into the device through a tube which produces a cloud of seed around the moving belts that is then entrained into the flow. This eliminates the possibility of biasing the data with artificial seeding velocities. FIND software, from TSI, was then used to statistically process the 50,000 samples obtained at each location. Data was velocity bias corrected according to the algorithm provided in FIND.

Numerical Method

A modified version of a subgrid model proposed earlier (refs. 8,9) is used in the present LES. The kinematic structure of premixed flames was investigated earlier (ref. 9). The model is extended here to include heat release. Within each LES cell, a representative one-dimensional domain is used to stochastically represent a local ray through the flame brush. The G-equation flame propagation model (refs. 9,10) is solved on this 1D line. The G-equation allows for propagation of the flame as a sharp front (negligible flame thickness) corresponding to a case of fast chemical kinetics (ref. 10). The effect of turbulent eddies on the species field is modeled stochastically using a scalar rearrangement process on segments chosen on the one-dimensional domain. More details is given elsewhere (refs. 9-12).

For heat release, the temperature is assumed to be a linear function of G. The obvious implication is that the transport and diffusive properties of the reactive scalar and the thermal energy are closely correlated (corresponding to a often used physical assumption of a constant Lewis number) in the subgrid domain. Transport of species and heat across LES cells is modeled using a "splicing" procedure (refs. 11,12). The thermodynamic pressure in each of the LES cells is assumed to be constant since it is well known that the second order reaction mechanisms do not cause a change in thermodynamic pressure across the flame. It is further assumed that the thermodynamic pressure is gradient free through out the physical domain. Any acoustic disturbance created by the flame is assumed at have small amplitude (zero Mach number approximation) and is communicated at infinite speed through out the domain. The LES-resolved temperature field can be obtained by filtering the local subgrid temperature fields. However, this procedure can lead to sharp discontinuity and hence, to numerical instability. Therefore, to locally smooth the LES-resolved temperature field (which is needed to close the LES equations), a diffusion equation for temperature is solved on the LES-grid at each LES time step using the subgrid-aveeraged field as an initial condition.

The numerical method is a fourth-order accurate finite-difference scheme in space and second order accurate in time. Since the thermodynamic pressure is constant, a zero Mach number version of the fractional step method (ref. 13) is used to integrate the LES equations.

Results and Discussion

Experimental Results: Figures 2a and 2b shows respectively, the mean and rms velocity distribution in the flow field. It can be seen that the profiles are not totally anti-symmetric. It was determined that this was due to an asymmetry in the end regions where the drive rollers are located and could not be avoided. However, this asymmetry did not appear to have any significant effect on the rms velocity. More importantly, the data shows a nearly constant rms fluctuations in the core which is of interest here. Figure 3 shows U^+ as a function of y^+. The data shows the expected behavior for a wall bounded shear flow. Both the viscous sublayer ($y^+<5$) and the inertial sublayer ($30<y^+<1000$) can be clearly observed. However, due to the noted asymmetry, the data at different Reynolds numbers do not exactly collapse as predicted by theory.

Figure 4 compares the measured streamwise fluctuations in various devices. The peak location in the present facility is in good agreement with earlier data but turbulence intensity magnitude is somewhat higher. This is probably due to the continuous nature of the flow and the compact nature of the device and is unavoidable here. Figure 5 compares the skin friction coefficient measured in this device to those in earlier devices. Deviations from the more ideal Couette flow are, once again, probably due to the recirculating nature of the flow in this compact device.

However, these results clearly establish that stationary turbulence with nearly constant turbulent fluctuations in the core of the flow exists in the present facility. Furthermore, the overall nature of the flow is in good agreement with theory and past studies in similar devices.

The experimental data can be utilized to estimate the resolved scales of motion. Using the belt spacing, h = 2.54 cm as the typical integral length, the Kolmogorov scale, η, is estimated in the core to be 0.23 mm for the Re_h = 4,366 case and 0.13 mm for the Re_h = 10,091 case. For the LDV system, the seed particle size is sub-micron, much smaller than η, while the LDV probe volume is of the order of η. This implies that the smallest scale can be nearly resolved. However, due to flow motion, the residence time inside the probe volume is a more accurate measure of the resolution. The velocity of the scale can be estimated by using the relation between Kolmogorov velocity scale and the magnitude of turbulent velocity: $u'/v = (Re_L)^{1/4}$. Based on the probe volume, a residence time and, therefore, a frequency 590Hz for the Re_h = 4,366 case and 1,030Hz for the Re_h = 10,091 case is estimated. This means that the data rate for the LDV should be greater than 2,060Hz to resolve Kolmogorov scales temporally. Because of the high noise levels in the system, this is difficult to achieve. Therefore, the best estimate is that the resolution is of the order of η. or larger.

These studies have clearly established the turbulent flow properties in this facility. Although hot flow studies cannot be carried out using this device (an identical hot flow facility is currently under construction), a preliminary study of buoyancy was carried out by using an excimer laser to ionize a small region of air in the flow. This produced a hot gas kernel that propagated into the flow. Using high speed Schlieren imaging, it was possible to observe the effects of shear caused by the Couette flow and the apparent distortion caused by buoyant stresses. This preliminary study suggested that buoyant effects should be observed in the actual reacting flow case. This is the focus of current study and the results will be reported in the near future.

Numerical Results: LES of non-reacting and reacting Couette flow corresponding to a Reynolds number (as defined earlier) of 10,000 have been conducted on a 49x49x33 grid. The mean velocity profile is compared with the corresponding result from the experiment in Fig 6. The LES profile is anti symmetric about the centerline whereas (as noted) there is some asymmetry in the experimental data. The rms velocity in the streamwise direction is compared to the experimental data in Fig. 7. The experiment indicates a peak in urms more closer to the wall than obtained in the LES. Assuming that the experimental results in such close vicinity of the moving belt are free of any error, one might be able to capture the peak in urms by increasing the near wall resolution. However, some uncertainty in the rms estimate is inevitable in the LES, since, the unresolved part of the turbulent kinetic energy (grid dependent) is captured only approximately as the subgrid kinetic energy. In any event, the propagation of the flame in the central core region with constant rms fluctuations is of interest in this study and this feature is captured here. Increase in the resolution in the core region captures the constant rms region more accurately, as shown earlier (ref. 9).

For reacting flows, the grid is rapidly stretched out from the wall but in the core region (mid 78%) a uniform grid is used to allow proper resolution of the propagating flame ball. The grid width is 10η in the core region and the simulation is stopped once the flame crosses this region. All simulations described here are for a reference u'/S_L of 4.0. Temperature rise factors of 4 and 7 were studied. Comparison with a model simulation using Yakhot's model for the turbulent flame speed (ref. 9) were also carried out to evaluate the predictions by the new subgrid LES method. Some representative results are reported below.

Five contours corresponding to equally spaced values of G between 0 and 1 are shown for each case in Fig. 8. As can be seen, the subgrid approach tends to capture the thin premixed flame quite well (usually within 2-3 grid points) when compared to conventional LES (i.e., solving the G-equation with the LES equations). As seen earlier (ref. 9), in the conventional approach significant numerical diffusion of the scalar gradients in G occurs and overwhelms the burning rate. This error is expected in all simulations that evolve the species equations on the LES grid using finite difference or finite volume schemes. Flame surface tracking methods can be implemented for cold flames but cause problems when heat release is added. The flame generates velocities normal to the flame surface because of the expansion behind it. The vertical currents are however curtailed by the presence of the wall, so the flow velocity tends to increase greatly in the streamwise and spanwise directions leading to flattening of the flame. A iso-level of G-surface corresponding to a value of 0.5 predicted by the subgrid approach is shown in Fig. 9. This figure shows visually an approximate shape of the wrinkled flame front.

To investigate the effect of gravity, two simulations (using the subgrid model) were conducted with heat release corresponding to a temperature ratio of 7.0. The first case is run with conditions corresponding to gravity on earth, the second with zero gravity. The density gradients caused due to heat release tend to compress the flame in the upper region and diffuse the flame in the lower regions in the presence of gravity. This is not very noticeable in the present simulations because of very high burning rate causing the flame to reach the wall very quickly. In Fig. 10, ten equally spaced contours of G at the same cross plane location are plotted for the cases with and without buoyancy. The whole flame tries to lift up in the presence of gravity due to buoyancy, although it is not very noticeable in the figure. However, it can be seen that the two simulations diverge in time indicating an observable buoyancy effect on premixed flames.

There are many structural and propagation properties of premixed flames that can be analyzed to characterize the flame structure. Figure 11 shows the pdf of the stretch in the plane of the flame (caused by flame curvature and rate-of-strain effects) for the two cases. Clearly, the flame structure under 1g exhibits increased positive stretch compared to the 0g case. Further study using finite-rate kinetics model is underway to understand the effect of buoyancy on such low Re turbulent premixed flames.

Conclusions

A facility in which turbulent Couette flow could be generated in a microgravity environment was designed and built. To fit into the NASA Lewis drop tower the device had to be very compact. This means that edge effects and flow re-circulation were expected to affect the flow. The flow was thoroughly investigated using LDV and was found to be largely two dimensional away from the edges with constant turbulence intensities in the core. Slight flow asymmetries are introduced by the non symmetric re-circulation of the fluid outside the test region. Belt flutter problems were remedied by adding a pair of guide plates to the belt. In general, the flow field was found to be quite similar to previously investigated Couette flows. However, turbulence levels and associated shear stresses were higher. This is probably due to the confined re-circulation zone reintroducing turbulence into the test section. An estimate of the length scales in the flow showed that the measurements were able to resolve nearly all the length scales of interest.

Using a new LES method for subgrid combustion it has been demonstrated that the new procedure is computational feasible even on workstation type environment. It is found that this model is capable of capturing the propagation of the premixed flames by resolving the flame in the LES grid within 2-3 grid points. In contrast, conventional LES results in numerical smearing of the flame and completely inaccurate estimate of the turbulent propagation speed. Preliminary study suggests that there is observable effect of buoyancy in the 1g environment suggesting the need for microgravity experiments of the upcoming experimental combustion studies.

With the cold flow properties characterized, an identical hot flow facility is under construction. It is assumed that the turbulence properties ahead of the flame in this new device will closely match the results obtained here. This is required since the hot facility will not enable LDV measurements. The reacting flow facility is also being constructed with planned drop tower experiments in mind. Therefore, issues related to safety and structural integrity are being take into account. Further development of the numerical model will also be carried out to include finite-rate kinetics for representative premixed cases. More detail analysis of the flame structure and propagation nature will be investigated. Simulations will also be compared to the flame properties observed in the experiments.

References

1. Williams, F. A., *Combustion Theory*, Second Edition., Addison-Wesley, New York, 1985.
2. Lekan, J., Gotti, D. J., Jenkins, A. J., Owens, J. C., Johnston, M. R., "User Guide for the 2.2 Second Drop Tower of the NASA Lewis Research Center," *NASA Technical Memorandum 107090*, 1996.
3. Aydin, E. M., and Leutheusser, H. J., "Plane-Couette flow between smooth and rough walls," *Experiments in Fluids*, Vol. 11, pp. 302-312, 1991.
4. Bech, K. H., Tillmark, N., Alfredsson, P. H., Andersson, H. I., " An Investigation of Turbulent Plane Couette Flow at low Reynolds Numbers," *Journal of Fluid Mechanics*, Vol. 285, pp. 291-325, 1995.
5. El Telbany, M. M. M., Reynolds, A. J., "The Structure of Turbulent Plane Couette Flow," *Journal of Fluids Engineering*, Vol. 104, pp. 367-372, 1982.
6. Robertson, J. M., and Johnson, H. F., "Turbulence Structure in Plane Couette Flow," *J. Eng. Mech.*, Proc. of Am. Soc. of Civil Engg., Vol. 6, pp. 1171-1182, 1970.
7. Clark, J. A., "A Study of Incompressible Turbulent Boundary Layers in Channel Flow," ASME *Journal of Basic Engineering*, Vol. 90, pp. 455-468, 1968.
8. Menon, S., McMurtry, P. A., and Kerstein, A. R., "A Linear Eddy Mixing Model for LES of Turbulent Combustion," in *LES of Complex Engineering and Geophysical Flows*, Galperin, B. and Orszag, S., eds., Cambridge University Press, pp. 287-314, 1993.
9. Menon, S. and Chakravarthy, V. K., Large-Eddy Simulations of Premixed Flames in Couette Flow, AIAA Paper No. 96-3077, 32nd AIAA/ASME/SAE/ASEE Joint Propulsion Conference, Lake Buena Vista, FL, July 1996.
10. Smith, T. and Menon, S., "Model Simulations of Freely Propagating Turbulent Premixed Flames", *Symposium (International) on Combustion*, 26, 1996 (to appear).
11. Menon, S and Calhoon, W., "Subgrid Mixing and Molecular Transport Modeling for Large-Eddy Simulations of Turbulent Reacting Flows", *Symposium (International) on Combustion*, 26, 1996 (to appear).
12. Calhoon, W. H. and Menon, S., "Linear Eddy Subgrid Modeling for Reacting Large-Eddy Simulations: Heat Release Effects," AIAA-97-0368, 35th Aerospace Sciences Meeting, Reno, NV, January 6-9, 1997.
13. Chakravarthy, K. and Menon, S., "On Large-Eddy Simulations of Non-Homogeneous Flows," AIAA 97-0652, 35th Aerospace Sciences Meeting Reno, NV, January 6-9, 1997.

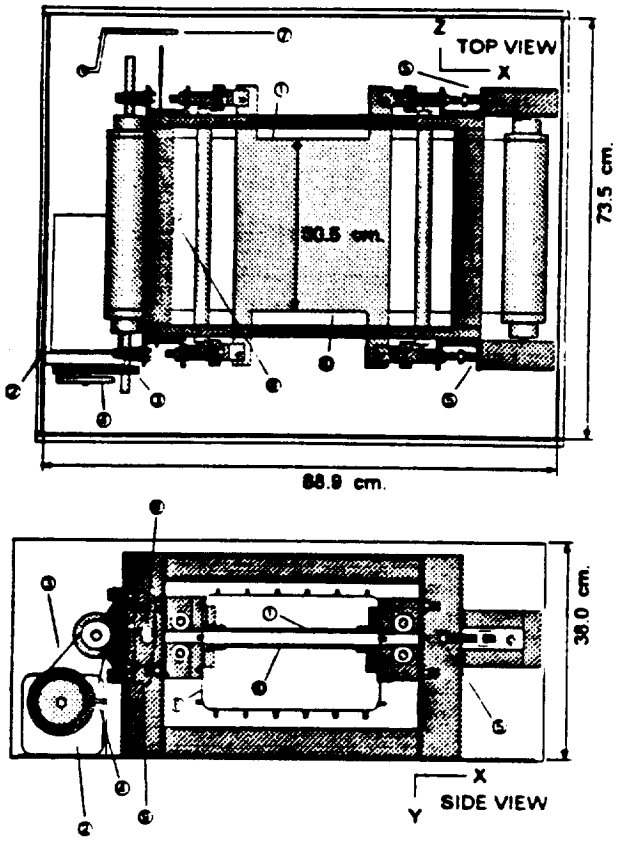

Figure 1. Setup of the experimental facility.

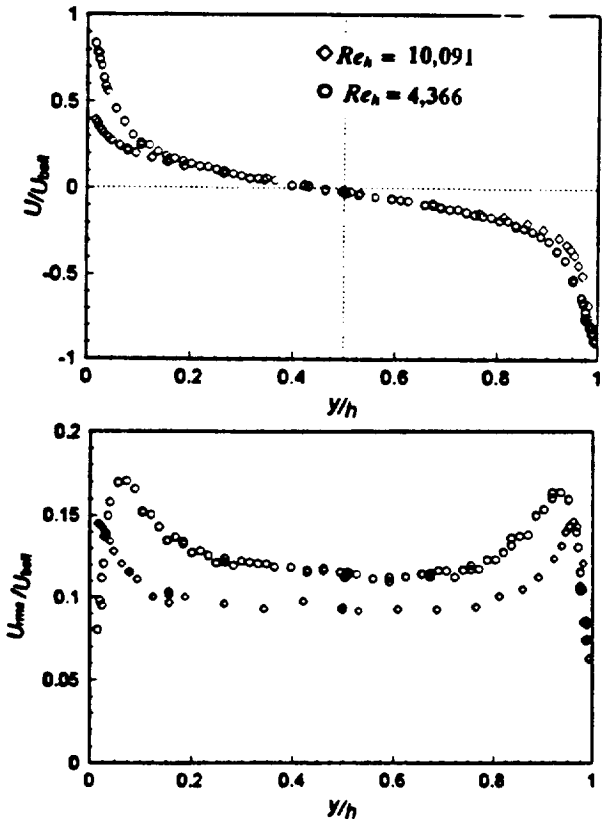

Figure 2. Mean (a) and rms (b) velocity fluctuations.

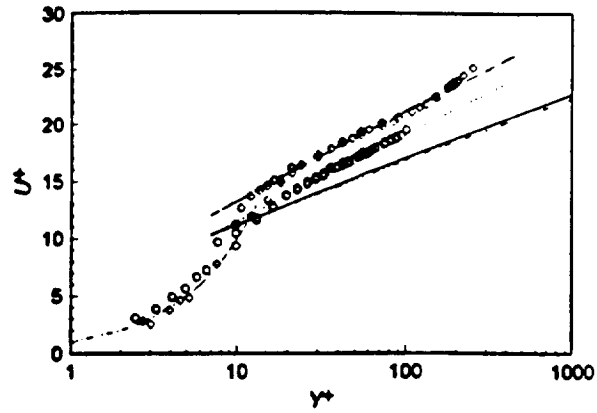

Figure 3. Non-dimensionalized near-wall velocity profile. Solid and dotted lines indicate curve fit to earlier data (refs. 3-7).

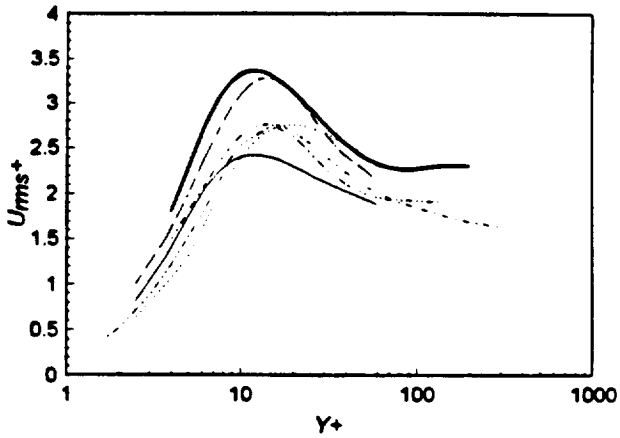

Figure 4. Comparison of present turbulence velocity fluctuation (shown as a bold line) with earlier experimental data (refs. 3-7).

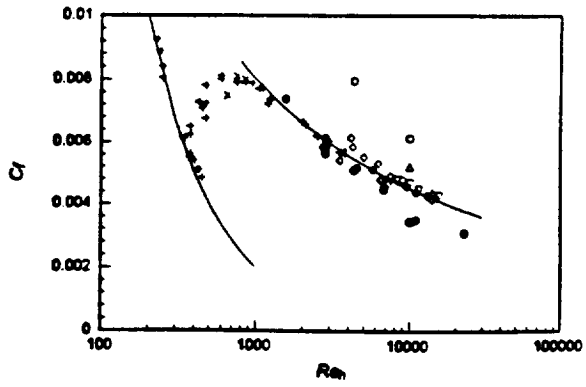

Figure 5. Skin friction coefficient comparison with earlier data. Solid circle: present study near wall; open circle: present study in the core. Other symbols correspond to data in refs. 3-7.

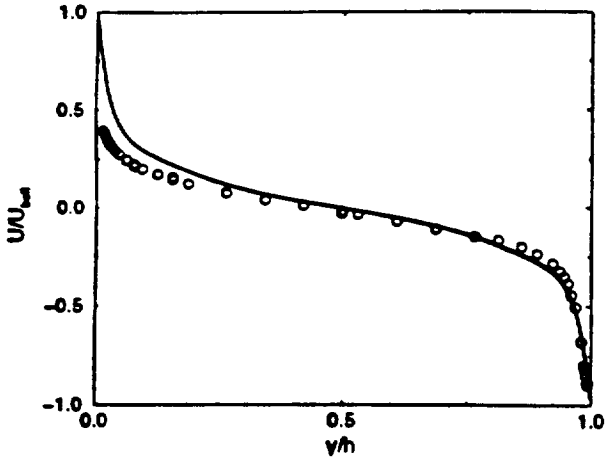

Fig.6:Mean velocity profiles
solidline:LES,symbols:expt.

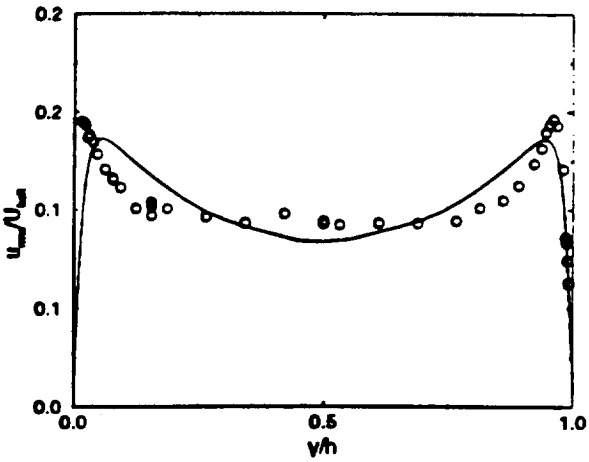

Fig.7:urms profiles
solidline:LES,symbols:expt.

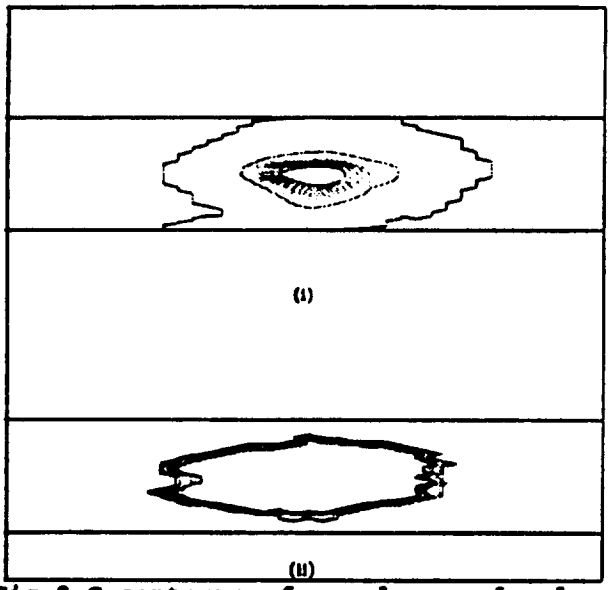

Fig.8:G-contours of equal spaced values
(i) Yakhot's model, (ii) LEM

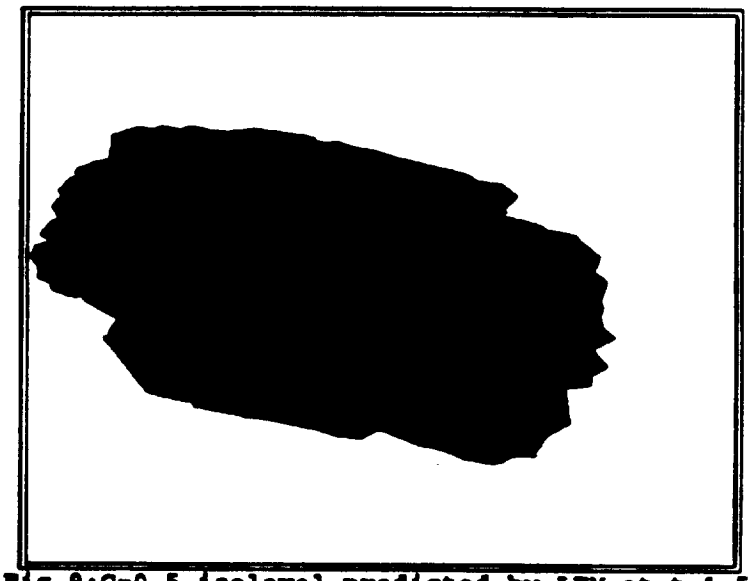

Fig.9:G=0.5 isolevel predicted by LEM at t=1.5
(t non-dimensionalized U_w and h)

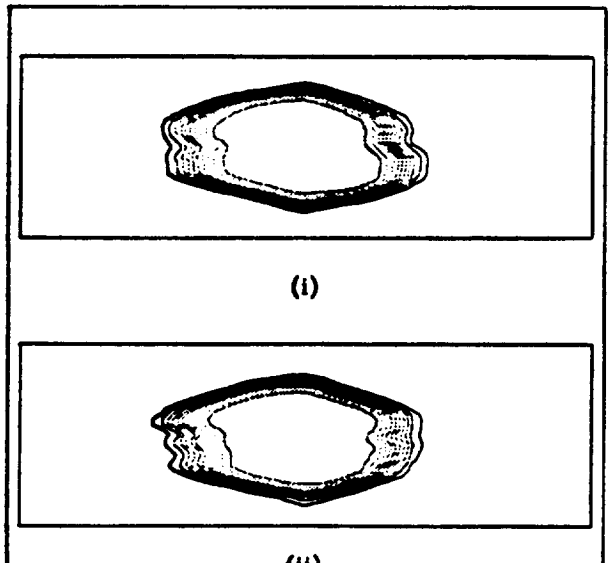

Fig.10:G-contours of equal spaced values
(i) zero gravity, (ii) gravity on earth

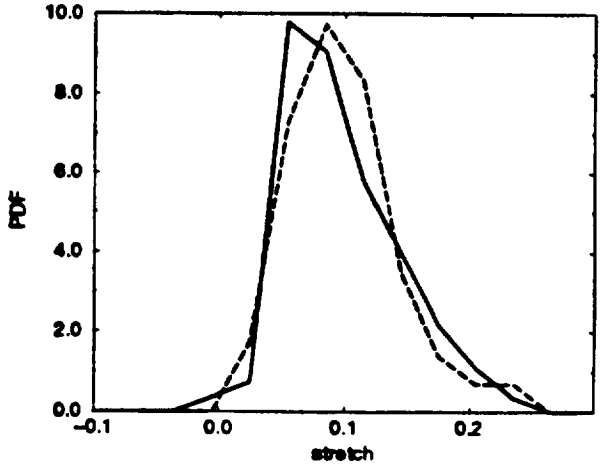

Fig.11:PDF of flame stretch
solid line: no gravity, dashed line:with gravity